Conference Paper, Published Version

Roulund, A.; Sumer, B. Mutlu; Fredsoe, J.; Michelsen, J.

3-D Numerical Modeling of Flow and Scour Around a Pile

3-D Numerical Modeling of Flow and Scour Around a Pile

By

A. Roulund[1], B.M. Sumer[2], J. Fredsøe[3], J. Michelsen[4]

ABSTRACT

A 3-D flow code, EllipSys3D, tested and validated, has been implemented along with a morphologic model to simulate the scour process around a vertical circular pile in a steady current in the case of non-cohesive sediment. The k-ω turbulence model has been used for closure. The morphologic model includes (1) a two-dimensional bed load sediment transport description, and (2) a description of surface-layer sand slides for bed slopes exceeding the angle of repose. The simulation captured all the bed features, i.e. the scour hole and the formation of a downstream dune at the initial stage, and the truncated cone-shaped scour hole in the equilibrium stage. The maximum equilibrium scour depth obtained from the simulation compares fairly well with the measurements.

INTRODUCTION

During the last 30 years, more than 1000 of about 600.000 bridges in the United States have failed, and 60% of those failures are due to scour, Briaud et al. (1999). More than 85.000 bridges in the U.S. are vulnerable to scour (about 80.000 being scour-susceptible and about 7.000 scour-critical) (Lagasse et al., 1995). Two excellent accounts of scour at bridge piers have recently appeared in the literature. One is a compendium of papers presented in the ASCE Water Resources Engineering Conferences from 1991 to 1998 with 371 abstracts and 75 papers (Richardson and Lagasse, 1999). The other is a book by Melville and Coleman (2000), which, along with the recent knowledge, draws on the experiences on scour in New Zealand, and illustrates a great many examples of case studies.

The present paper deals with scour around a vertical circular pile in steady currents. The key element in the scour process is the so-called horseshoe vortex (Fig. 1). This vortex, combined with the effect of the contraction of streamlines at the side edges of the pile (Fig. 1), can erode a significant amount of sediment away from the neighbourhood of the pile, leading to a truncated-cone-shaped scour hole around the pile.

[1] Technical University of Denmark, Department of Mechanical Engineering, Coastal and River Engineering Section, Building 115, 2800 Lyngby, Denmark. Present address: NIRAS Sortemosevej 2, 3450 Allerød, Denmark
[2] Technical University of Denmark, Department of Mechanical Engineering, Coastal and River Engineering Section, Building 115, 2800 Lyngby, Denmark, (sumer@isva.dtu.dk)
[3] The same as above.
[4] Technical University of Denmark, Department of Mechanical Engineering, Fluid Mechanics Section, Building 403, 2800 Lyngby, Denmark.

Scour around piles in steady currents has been investigated quite extensively (particularly in the context of scour at bridge piers). Reviews of the subject can be found in the books of Breusers and Raudkivi (1991), Hoffmans and Verheij (1997), Whitehouse (1998), Raudkivi (1998), Melville and Coleman (2000) and Sumer and Fredsøe (2002).

While much has been written on the subject of scour around piles in steady currents, comparatively few studies have been presented of the 3-D numerical modeling of scour. Table 1 gives a list of studies on the 3-D modeling of flow and scour around piles in steady currents. As seen from the table, Olsen and his co-workers (1993, 1998) were the only researchers to undertake the 3-D modeling of the actual scour process.

The purpose of the present study is (1) to implement a hydrodynamic model, EllipSys3D, for the 3-D flow around a pile, both with a rigid plane bed and with a sediment bed undergoing scour; and (2) to conduct a 3-D numerical simulation of the actual scour process itself, using the former hydrodynamic model. A major paper, which summarizes the results of the study, is under preparation, Roulund et al. (2002). The present paper reports some of the results obtained for the numerical simulation of the scour process in the case of steady current.

HYDRODYNAMIC MODEL

A three-dimensional general-purpose flow solver, EllipSys3D, has been used to calculate the flow. EllipSys3D is a finite volume numerical model that solves the incompressible Reynolds-averaged Navier-Stokes equations

$$\frac{\partial \rho U_i}{\partial t} + \frac{\partial \rho U_i U_j}{\partial x_j} = -\frac{\partial p}{\partial x_i} + \frac{\partial}{\partial x_j}\left[(\mu + \mu_T)(\frac{\partial U_i}{\partial x_j} + \frac{\partial U_j}{\partial x_i}) \right] \quad (1)$$

in which U_i is the i-th component of velocity; t is the time; x_i is the Cartesian coordinates; ρ is the fluid density; p is the dynamic pressure; μ is the viscosity; and μ_T is the eddy viscosity, calculated by a two-equation eddy-viscosity type turbulence model, as detailed in the following paragraphs.

EllipSys3D has been developed at the Risø National Laboratory, Denmark and at the Technical University of Denmark. It is an incompressible general purpose Navier-Stokes solver. It is basically a multiblock finite volume discretisation of the Reynolds Averaged Navier-Stokes equations. A Variety of turbulence models are available. The model is under constant development. It has been implemented successfully in various engineering problems such as those in wind engineering and aeronautical engineering. The basic principles of the model have been described in Sørensen, 1995 and Michelsen, 1992. The following web address can be consulted for further information:
http://www.risoe.dk/vea-aed/numwind/ellipsys.htm

We have also implemented the model to simulate the flow around and forces on a sphere placed near a bed. A paper summarizing the results of this latter study is under preparation.

For steady-state flow calculations, the SIMPLE algorithm (Patankar, 1980) is used. In this algorithm, the pressure field is calculated and the velocity field is corrected so that the continuity equation

$$\frac{\partial \rho}{\partial t} + \frac{\partial \rho U_j}{\partial x_j} = 0 \tag{2}$$

is satisfied in an iterative manner. By underrelaxation of the correction to the velocity field, the transient components of the flow are suppressed. Although the majority of the present study involved steady-state flow calculations, some transient flow calculations have also been performed.

Table 1. A list of studies on 3-D modeling of flow and scour around a pile in a current.

Author	Turbulence model	Steady current: Steady solution; or Transient solution	Bed: Rigid bed; or Sediment bed	Scour	Remarks
Olsen and Melaaen (1993)	k-ε	Steady solution	Sediment bed	Initial stage of scour is simulated. Clear-water scour	Horseshoe vortex is resolved
Olsen and Kjellesvig (1998)	,,	,,	,,	Entire scour process is simulated. Clear-water scour	,,
Richardson and Panchang (1998)	Turbulent closure through a number of advanced schemes	Steady solution, and Transient solution (?)	Three kinds of "frozen" rigid beds, ranging from a plane bed to equilibrium scour hole	Scour process is not simulated	,,
Tseng, Yen and Song (2000)	Large Eddy Simulation	Transient solution	Rigid plane bed	Scour process is not simulated	Horseshoe vortex and vortex shedding are resolved
Present	k-ω	Steady solution, and Transient solution	Both rigid and sediment beds	Entire scour process is simulated. Live-bed scour	Horseshoe vortex is resolved. Vortex shedding is resolved in some rigid-bed simulations

The k-ω model (Wilcox, 1993) has been selected as the turbulence model because of its better performance in the case of boundary-layer flows with strong adverse pressure gradients (Wilcox, 1993; Menter, 1992). The details of (1) the algorithms used in both the steady-state flow calculations and the transient calculations and (2) the turbulence model adopted in the study will be given in Roulund et al. (2002).

The boundaries of the computational domain are (1) Inlet, (2) Outlet, (3) Symmetry Boundaries and (4) Walls.

At the inlet boundary, zero transverse, v, and vertical, w, velocities were specified. The inlet profiles for u, k and ω were based on the equilibrium profiles obtained from uniform-channel flow calculations with similar flow settings. At the outlet boundary, zero-gradient (Neumann) conditions were applied for all quantities. At the symmetry boundaries (i.e., at the sides and top surface of the computational domain), Neumann conditions were applied for k and ω, while no-flux conditions were applied for the three components of the velocity, u, v and w (in which u is the streamwise component of the velocity). At the walls (i.e., at the bed, and at the surface of the pile) zero velocity was specified for u, v and w; zero turbulent energy was specified for k when the wall was smooth, while the Neumann condition was applied when the wall was rough and transitional. Regarding the latter condition, experiments do reveal that the Neumann condition (i.e., $\partial k/\partial n = 0$) is satisfied at the wall, n being the direction normal to the wall; see Nezu, 1977; Sumer et al., 2001 and 2002). The Dirichlet condition was applied for ω,

$$\omega = S_r \frac{{U_f}^2}{\upsilon} \tag{3}$$

in which $U_f = (\tau_0 / \rho)^{1/2}$ is the friction velocity based on the wall shear stress τ_0. The quantity S_r is a tuning parameter, and it is used to account for the bed roughness:

$$S_r = (\frac{40}{{k_s}^+})^3, \quad {k_s}^+ < 20.2 \tag{4}$$

$$S_r = \frac{100}{({k_s}^+)^{0.85}}, \quad {k_s}^+ > 20.2 \tag{5}$$

in which ${k_s}^+ = k_s U_f / \nu$ is the wall roughness in wall units, ν is the kinematic viscosity and k_s is Nikuradse's equivalent sand roughness. Wilcox (1993) was the first to introduce the previous boundary condition. The tuning parameter S_r was given by Wilcox (1993) in a form slightly different from that in the preceding equations.

The momentum, continuity and turbulence-model equations are transformed into curvilinear coordinates, linearised and decoupled. The latter has been described in detail in Sørensen (1995), following the principles given in Patankar (1980).

The computational mesh is based on a multi-block structure with each block containing N^3 computational cells where N is the number of cells in each spatial direction. $N = 16$ was used for the scour and transient-flow simulations. The total number of cells in these cases was 197.000. The number of cells across the depth was 32, and the number of cells around the pile perimeter was 64. The length, width and depth of the computational domain were 15D, 18D and 2D, respectively. In the case of steady (not transient) rigid-bed simulations, N was 32; the total number of cells was 786.000; the number of cells across the depth was 64, while the number of cells around the pile perimeter was 128; the length, width and depth of the computational domain were 20D, 20D and 2D,

respectively. (It may be noted that N = 32 required prohibitively large computational times for the scour and transient flow simulations). Fig. 2 shows a detailed picture of the mesh used for the steady-current rigid-bed calculations.

MORPHOLOGIC MODEL

The morphologic model couples the flow solution with a sediment transport description, and routines for updating the computational mesh based on the mass balance of sediment.

There are three elements in the morphologic model: (1) the bed load; (2) the sand slide; and (3) the equation of continuity for sediment.

Each element is now considered individually.

Bed load. A two-dimensional bed load description has been developed. This description is actually an extension of the bed-load equation of Engelund and Fredsøe (1976) to a 2-D vectorial representation. The bed load occurs on a slope (Fig. 3). $\overrightarrow{U_b}$ is the mean transport velocity of a particle moving as bedload. The fluid velocity at the particle position is $\vec{U}$, different from $\overrightarrow{U_b}$ (Fig. 3). Following Engelund and Fredsøe (1976), the latter velocity may be taken as $\vec{U} = a\overrightarrow{U_f}$ in which $\overrightarrow{U_f}$ is the friction velocity, and a is an empirical constant, taken as a = 10.

The rate of bedload transport in volume per unit time and per unit width, $\overrightarrow{q_b}$, is related to $\overrightarrow{U_b}$ by the following equation (Engelund and Fredsøe, 1976)

$$\overrightarrow{q_b} = \frac{\pi}{6} d^3 \frac{p_{EF}}{d^2} \overrightarrow{U_b} \tag{6}$$

in which d is the grain size, and p_{EF} is the percentage of particles in motion in the surface layer of the bed. The above equation implies that the bedload transport is determined by two quantities: p_{EF} and $\overrightarrow{U_b}$.

In the case where the sediment transport takes place on a horizontal bed, Engelund and Fredsøe (1976) obtained the following semi-empirical expression for p_{EF}

$$p_{EF} = \left[1 + \left(\frac{\frac{\pi}{6}\mu_d}{\theta - \theta_c} \right)^4 \right]^{-1/4} \tag{7}$$

in which μ_d is the dynamic friction coefficient, taken as 0.51 (Fredsøe and Deigaard, 1992, p. 218), θ is the Shields parameter and θ_c is the critical value of θ for the initiation of sediment motion at the bed.

We have adopted in the present study the same expression as in Eq. 7 to calculate the quantity p_{EF}. In the case of the sloping bed, p_{EF} may undergo a slight change, in the order of magnitude of (1/cos β) where β is the slope of the bed (Fig. 3). However, this has not been incorporated in the calculations on grounds that such a refinement in the model may be inconsistent with several other assumptions inherent in the formulation of the sediment transport.

The Shields parameter in Eq. 7 is

$$\theta = \frac{{U_f}^2}{g(s-1)d} \tag{8}$$

in which s is the specific gravity of the sediment grains, and g is the acceleration due to gravity. U_f in Eq. 8 is taken as the magnitude of the friction-velocity vector associated with the skin friction.

The critical Shields parameter in Eq. 7, on the other hand, is

$$\theta_c = \theta_{c0}(\cos\beta\sqrt{1-\frac{\sin^2\alpha\tan^2\beta}{{\mu_s}^2}}-\frac{\cos\alpha\sin\beta}{\mu_s}) \tag{9}$$

in which θ_{c0} is the critical Shields parameter for a horizontal bed, taken as 0.05, μ_s is the static friction coefficient, taken as $\mu_s = 0.63$ for the sand used in the present simulation (Lambe and Whitman, 1969, p.149), and α is the angle between the flow velocity vector and the direction of the steepest bed slope (Fig. 3).

The particle velocity is obtained from the two components of the equation of particle motion. The equation of motion in the direction of particle motion, considering that the particle is, on average, moving with a constant velocity:

$$F_D\cos\psi_1 + W\sin\beta\cos(\alpha-\psi) - (W\cos\beta)\mu_d = 0 \tag{10}$$

in which W (= $(\pi/6)\rho g(s\text{-}1)d^3$) is the submerged weight of the particle, F_D is the drag force

$$F_D = \frac{1}{2}\rho C_D\frac{\pi}{4}d^2{U_r}^2 \tag{11}$$

in which C_D is the drag coefficient, and U_r is the velocity of the fluid (at the particle position) relative to the particle (Fig. 3), $\overrightarrow{U_r} = a\overrightarrow{U_f} - \overrightarrow{U_b}$. Luque (1974) (see also Fredsøe and Deigaard, 1992, p. 211) found from his experiments:

$$C_D = \frac{4\mu_s}{3a^2(\frac{1}{2}\theta_{0c})} \tag{12}$$

The equation of motion in the direction perpendicular to $\overrightarrow{U_b}$, on the other hand, reads:

$$F_D \sin\psi_1 - W \sin\beta \sin(\alpha - \psi) = 0 \tag{13}$$

There are also the following geometric relations from Fig. 3

$$U_r \sin\psi_1 - aU_f \sin\psi = 0 \tag{14}$$

and

$$U_r \cos\psi_1 - aU_f \cos\psi + U_b = 0 \tag{15}$$

Eqs. 10, 13, 14 and 15 are to be solved for the four unknown quantities, namely U_b, U_r, ψ and ψ_1. Once U_b and ψ_1 are determined (and therefore $\overrightarrow{U_b}$ is obtained), then inserting $\overrightarrow{U_b}$ and p_{EF} in Eq. 6 will give the bed load transport $\overrightarrow{q_b}$.

Sand slide. Observations show that, during the development of the scour process, there are areas at the upstream side of the scour hole where the local bed slope exceeds the angle of repose, and, as a result, shear failures occur at these locations. Two "ingredients" of this latter process are that, first of all, the backward flow at the base of the pile erodes the foot of the upstream slope of the scour hole (A in Fig. 4), and secondly there is a continuous sediment supply into the scour hole from upstream (B in Fig. 4).

Our visual observations have indicated that, in the upstream part of the scour hole, the bed "avalanched" when the slope β exceeded approximately the angle of repose, $\beta_r = 32^0$, by a few degrees. They have also shown that this shear failure of the soil occurred just below the bed surface, and sand slided down towards the centre of the scour hole, and, after each sand slide, the bed slope was a few degrees lower than the angle of repose.

Based on these observations, a sand slide procedure was developed to calculate the new slope of the bed, and it was incorporated in the morphologic model. The adopted procedure is as follows: (1) Calculate a new sediment transport rate when the local bed slope is exceeded $\beta_r + 2^0$. (2) Do this, based on a new particle velocity U_b, obtained from the following equation:

$$W \sin\beta - \mu_d W \cos\beta - \frac{1}{2}\rho C_D \frac{\pi}{4} d U_b{}^2 = 0 \tag{16}$$

(This is basically the equation of motion for a sediment particle (undergoing the sand slide) in the direction of the particle motion, considering that the particle is, on average, moving with a constant velocity in an otherwise still water). (3) Update the bed with the ordinary morphology scheme (described in the following paragraphs). (4) Repeat this procedure until the local bed slope was reduced to $\beta_r - 2^0$. In this procedure, a pseudo time step was used since it was assumed that the sand slide takes place instantaneously.

Continuity equation for sediment. The mass balance for sediment at each grid point on the bed is

$$\frac{\partial h}{\partial t} = \frac{-1}{1-n} \frac{1}{A} \sum_{i=1}^{4} (\overrightarrow{q_{b,i}} \bullet \overrightarrow{n_i}) |l_i| \tag{17}$$

in which h is the bed elevation, n is the porosity (taken as n = 0.4 in the present calculations); A is the projected area (on the x,y plane) of a small bed element; i indicates the number assigned to each side of the projected area (i=1,..4); $\vec{n}_i$ are the normal vector at the i–th side of the projected area, $\overrightarrow{q_{b,i}}$ is the sediment transport vector at the i–th side of the projected area; and $|l_i|$ is the length of the i–th side of the bed element.

The procedure in the computations was as follows: (1) Generate the mesh; (2) Calculate the flow; (3) Calculate the sediment transport due to bed load; (4) Update the bed; (5) Check the sand slide; and (6) Return Step 1. The morphological time step in the calculations was 0.02 s initially, and gradually raised to 0.1 s. The computational time was 2.5 months on an Alpha 21264 workstation, equivalent to a 1500 MHz Pentium IV.

Finally, it may be noted that, in the present model, the sediment transport is taken as the bed load alone (no suspended-load sediment transport is considered). To the authors' knowledge, no study is yet available, investigating the effect of the suspended load on scour in a systematic manner. However, the data reported in Baker (1986) (where the velocity is increased gradually so as to cover the flow regimes from the clear-water scour to the live-bed scour with the bed-load, the bed-load and suspended load and finally the suspended-load mode sheet-flow regimes; see Melville and Sutherland, 2000, p. 493, or Sumer and Fredsøe, 2002, p. 179) suggests that this effect is not radically significant.

RESULTS AND DISCUSSION

A detailed validation exercise has been undertaken for the hydrodynamic model for the case where the bed was plane and rigid. Three kinds of quantities have been tested, namely the velocity, the pressure and the bed shear stress. The velocities calculated by the model have been compared with our own data, obtained with the Laser Doppler Anemometry technique. (This has been achieved for both smooth and rough bed cases). The pressures have been calculated for the same test conditions as in the experiments of Dargahi (1989) and compared with the measured pressures of the latter author. The bed shear stresses, calculated from the model, have been compared with our own hot-film measurements, and also with the experimental data of Hjorth (1975) where the bed shear stress was measured, again, using the hot-film technique. A detailed description of the entire validation exercise including the description of the experiments will be given in Roulund et al. (2002).

From the latter, it has been concluded that the model captures fairly well the mean features of the 3-D flow, including the horseshoe vortex (one of the key elements in the scour process), meaning that it can be used for the calculation of the scour process around a pile placed in a sediment bed. The following paragraphs will present the results of this numerical experiment where the scour process is simulated using the previously described hydrodynamic and morphologic model.

In the numerical simulation of scour, vortex shedding was not resolved (the steady-state flow simulation was adopted). This was because of the prohibitively large computational

times required for the transient flow solution (where the vortex shedding is resolved) combined with the time-resolved morphologic calculations. We shall return to this point later in the section.

The water depth in the simulation was taken as δ =20 cm, corresponding to the boundary layer thickness. The pile diameter was D = 10 cm. The mean flow velocity was V = 46 cm/s. Based on the mean grain size d_{50} = 0.26 mm, Nikuradse's equivalent sand roughness for the bed was estimated to be k_s = 0.7 mm from the relation $k_s = 2.5\ d_{50}$. The Shields parameter was θ = 0.11, i.e., the scour was in the live bed regime. The ratio between the approach velocity and the critical velocity for the initiation of sediment motion was V/V_c = 1.6.

In the simulation, the bed ripples were resolved. To trigger the development of ripples a perturbation was applied to the prescribed bed roughness in the first 20 seconds of the simulation. The sediment transport description in the present model is based on uniform-size sand, i.e., the sediment gradation was $\sigma_g = d_{85}/d_{50} = 1$.

Fig. 5 shows a sequence of pictures, illustrating the time evolution of the scour hole obtained in the present simulation. As seen from the figure, all the topographic bed features observed in a typical scour process (in the laboratory, or in the field, see for example, Melville and Coleman, 2000 and Sumer and Fredsøe, 2002) are captured. These features are: (1) The semi-circular shape of the upstream part of the scour hole with a slope equal to the angle of repose; (2) The formation of a "bar" downstream of the pile (the deposited sand), and its downstream migration; (3) The formation of a gentler slope of the downstream side of the scour hole; and (4) The formation and migration of ripples outside the scour hole.

Baker (1986) (see also Melville and Coleman, 2000, p. 493) reports experimental data for the equilibrium scour depth as a function of the sediment gradation σ_g and the velocity ratio V/V_c. For V/V_c = 1.25 (the value of the velocity ratio used in the simulation), the experimental data for the equilibrium scour depth can be worked out from the data reported in the latter publications. Table 2 (Row 2) presents the results of this exercise.

Table 2. Equilibrium scour depths for V/V_c = 1.25. Comparison. The experimental values in the second row in the table are worked out from the experimental data of Baker (1986) (see also Melville and Coleman, 2000, p. 493 for Baker's data).

Sediment gradation, σ_g	1.0	1.3	2.3	2.9	4.4	5.2
Equilibrium scour depth, S/D Experiments, δ/D = 3.8-6, Baker (1986)	-	1.9	1.7	0.9	0.4	0.16
Equilibrium scour depth, S/D Numerical result, δ/D = 2, Present	1.5	-	-	-	-	-

Table 2 shows that the normalized equilibrium scour depth S/D for a sediment with a size distribution close to uniform, namely σ_g = 1.3, is S/D =1.9. The present simulation (for sediment with a uniform size distribution) predicts this value as S/D = 1.5 (21% smaller

than the measurements for σ_g = 1.3). It may be noted, however, that part of this discrepancy may be accounted for the relatively small value of the boundary-layer-to-pile-diameter ratio in the simulation, namely $\delta/D = 2$ (see Melville and Sutherland, 1988, for the influence of the boundary-layer thickness on the scour depth; see also Sumer and Fredsøe, 2002, p. 180).

Fig. 6 shows the bed shear stress amplifications for the initial plane bed and for the equilibrium scoured bed in the simulation. The bed shear stress amplification for the scoured bed is reduced considerably. However, the bed shear stress in the scour hole is still larger than outside the scour hole. This is linked to the relatively higher transport rates inside the scour hole (the higher transport rates dictated by the sediment continuity).

As discussed earlier, the vortex shedding is not resolved in the present scour calculations. To observe the influence of the vortex shedding on the flow, some transient flow calculations with a rigid plane bed have been undertaken. These calculations have shown the following. (1) The transient behaviour of the wake was evident from the numerical simulation with the shear layers emanating from the side edges of the pile, rolling up to form the lee-wake vortices sketched in Fig. 1, which eventually lead to vortex shedding; (2) The horseshoe vortex was also evident in the transient calculations (not surprisingly); and (3) The transient component of the flow regarding the horseshoe vortex was practically nonexistent; the present simulation did not resolve the secondary, time-dependent vortices within the horseshoe vortex reported in Baker (1979) and Dargahi (1989).

In the previously described steady-state solutions of the present flow model, the transient component of the flow is suppressed in the iteration procedure of the numerical simulations (see the discussion under Hydrodynamic Model above). In this connection, an interesting question may be: how does the steady solution compare with that obtained by *time averaging of the transient solution* (the time averaging taken over one vortex-shedding period). Fig. 7a shows the contour plot of the bed shear stress obtained from the steady solution, while Figure 7b shows that of the time-averaged bed shear stress from a transient simulation. As seen, the two plots are almost identical. It is only in the wake region where a slight difference is observed. This would enable the large computational times for transient simulations to be reduced tremendously (by as much as an order of magnitude) by adopting steady simulations of the flow, and obviously the latter would be a great advantage when such computations are implemented for scour calculations.

CONCLUSIONS

1. A 3-D hydrodynamic model, EllipSys3D, incorporated with the k-ω turbulence model has been adopted to simulate the flow around a vertical circular pile exposed to a steady current.
2. The model has been coupled with a morphologic model. The latter has been used to calculate scour around a vertical circular pile exposed to a steady current.
3. The present numerical simulation captures all the main features of the scour process.

4. The equilibrium scour depth obtained from the simulation agrees fairly well with the measurements.
5. The calculations show that the amplification in the bed shear stress around the pile is reduced considerably with respect to that experienced at the initial stage where the bed is plane.
6. The calculations also show that the bed shear stress in the scour hole can still be larger than the undisturbed value. This is linked to the contraction of the streamlines in the scour hole towards the pile.
7. Computations with a rigid plane bed reveal that the steady flow calculations give practically the same bed shear stress as the time-averaged bed shear stress obtained from the transient flow calculation.

ACKNOWLEDGEMENTS

This study has been partially funded by the Commission of the European Communities, Directorate-General XII for Science, Research and Development Program Marine Science and Technology (MAST III) Contract No. MAS3-CT97-0097, Scour Around Coastal Structures (SCARCOST), and by the five-year (1999-2004) Framework Programme "Computational Hydrodynamics" of the Danish Technical Research Academy, STVF.

REFERENCES

1. Baker, C. J. (1979). "The laminar horseshoe vortex". J. Fluid Mechanics, vol. 95, part 2, 347-367.
2. Baker, R. A. (1986). Local Scour at Bridge Piers in Non-Uniform Sediment. Thesis presented to the University of Auckland, New Zealand, in partial fulfillment of the requirements for the degree of Master of Philosophy.
3. Breusers, H.N.C. and Raudkivi, A.J. (1991). Scouring. A.A. Balkema, Rotterdam, viii + 143 p.
4. Briaud, J.-L., Ting, F.C.K., Chen, H.C., Gudavalli, R., Perugu, S. and Wei, G. (1999). "SRICOS: Prediction of scour rate in cohesive soils at bridge piers". *J. Geotechnical and Geoenvironmental Engineering*, ASCE, vol. 125, No. 4, 237-246.
5. Dargahi, B. (1989). "The turbulent flow around a circular cylinder". *Exp. in Fluids*, vol. 8, 1-12.
6. Engelund, F. and Fredsøe, J. (1976). "A sediment transport model for straight alluvial channels". *Nordic Hydrology*, vol. 7, 293—306.
7. Fredsøe, J. and Deigaard, R. (1992). Mechanics of Coastal Sediment Transport, World Scientific, xx + 369 p.
8. Hjorth, P. (1975). Studies on the nature of local scour. Bull. Series A, No. 46, viii + 191 p., Department of Water Resources Engineering, Lund Institute of Technology/University of Lund, Lund, Sweden.
9. Hoffmans, G.J.C.M. and Verheij (1997). Scour Manual. A.A. Balkema/ Rotterdam.
10. Lagasse, P.F., Thompson, P.L. and Sabol, S.A. (1995). "Guarding against scour". *Civil Engineering*, June issue, 56-59.
11. Lambe T.W. and Whitman, R.V. (1969). Soil Mechanics. John Wiley and Sons, Inc.
12. Luque R.F. (1974). Erosion and Transport of Bed Sediment, Dissertation, Jrips Repro B.V.-Meppel.
13. Melville, B.W. and Coleman, S.E. (2000). Bridge Scour. Water Resources Publications, LLC, CO, USA, xxii + 550 p.
14. Melville, B.W. and Sutherland, A.J. (1988). "Design methods for local scour at bridge piers". *J. Hydraulic Engineering, ASCE*, vol. 114, No. 10, 1210-1226.
15. Menter, F.R. (1993). "Zonal two equation k-ω turbulence models for aerodynamic flows". AIAA-paper-93-2906, *AIAA 24th Fluid Dynamic Conference*, July 6-9, 1993, Orlanda, Florida.

16. Michelsen, J.A. (1992). Basis3D - a platform for development of multiblock PDE solvers. Technical report, Dept. of Fluid Mechanics, Technical University of Denmark, AFM 92-05, ISSN 0590-8809.
17. Nezu, I. (1977). Turbulent Structure in Open Channel Flows. Ph.D. thesis, Kyoto University, Japan.
18. Olsen, N.R.B. and Kjellesvig, H.M.(1998). "Three-dimensional numerical flow modelling for estimation of maximum local scour", *J. Hydr. Res*., 36(4), 579-590.
19. Olsen, N.R.B. and Melaaen, M.C. (1993). "Three-dimensional calculation of scour around cylinders". *J. Hydraulic Engineering, ASCE*, vol. 119, No. 9, 1048-1054.
20. Patankar, S.V. (1980). Numerical Heat Transfer and Fluid Flow. Series in computational methods in mechanics and thermal sciences, Taylor and Francis.
21. Raudkivi, A.J. (1998). Loose Boundary Hydraulics. A.A. Balkema / Rotterdam.
22. Richardson, E.V. and Lagasse, P.F. (1999). Stream Stability and Scour at Highway Bridges. Compendium of Papers ASCE Water Resources Engineering Conferences 1991 to 1998. Richardson and Lagasse (eds.). ASCE, 1801 Alexander Bell Drive, Reston, Virginia 20191-4400. xxxi + 1040 p.
23. Richardson J.E. and Panchang V.G. (1998). "Three-dimensional simulation of scour-inducing flow at bridge piers", *J. Hydraulic Engineering, ASCE*, vol.124, No. 5, 530-540.
24. Roulund, A., Sumer, B.M. and Fredsøe, J. (2002). "Numerical and Experimental investigation of flow and scour around a circular pile". Manuscript in preparation.
25. Sumer, B.M. and Fredsøe, J. (2002). Mechanics of Scour in the Marine Environment. World Scientific, xiv + 536 p.
26. Sumer, B.M., Cokgor, S. and Fredsøe, J. (2001). "'Suction removal of sediment from between armour blocks". *J. Hydraulic Engineering, ASCE*, vol. 127, No. 4, pp. 293-306.
27. Sumer, B.M., Chua, L.H.C., Cheng, N.-S. and Fredsøe, J. (2002). "The influence of turbulence on bedload sediment transport". Manuscript submitted.
28. Sørensen, N.N. (1995). General purpose flow solver applied to flow over hills. Ph.D. thesis, Risø National Laboratory, Roskilde, Denmark, Risø-R-827(EN).
29. Tseng, M.-H., Yen, C.-L. and Song, C.C.S. (2000). "Computation of three-dimensional flow around square and circular piers". *International J. for Numerical Methods in Fluids*, vol. 34, 207-227.
30. Whitehouse, R. (1998): Scour at Marine Structures. Thomas Telford, xix + 198 p.
31. Wilcox, D.C. (1993). Turbulence modeling for CFD. DCW Industries, Inc, La Canada, California, USA, 2nd edition.

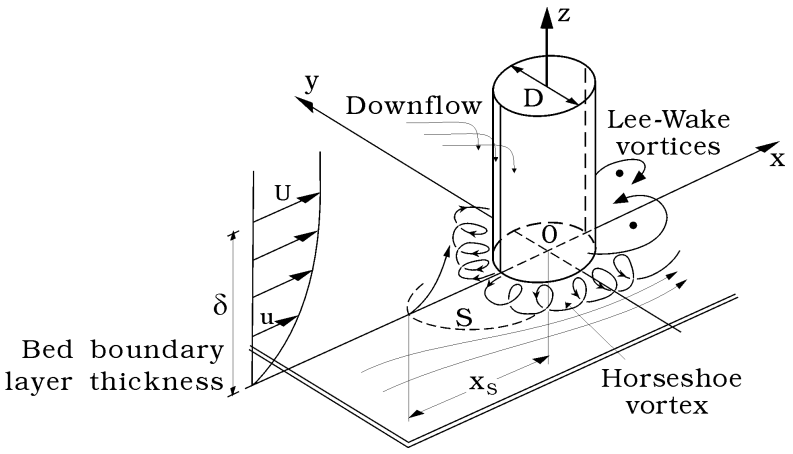

Fig. 1. Definition sketch.

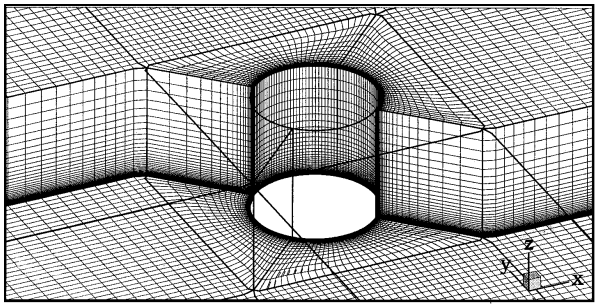

Fig. 2. Detail of mesh and block structure.

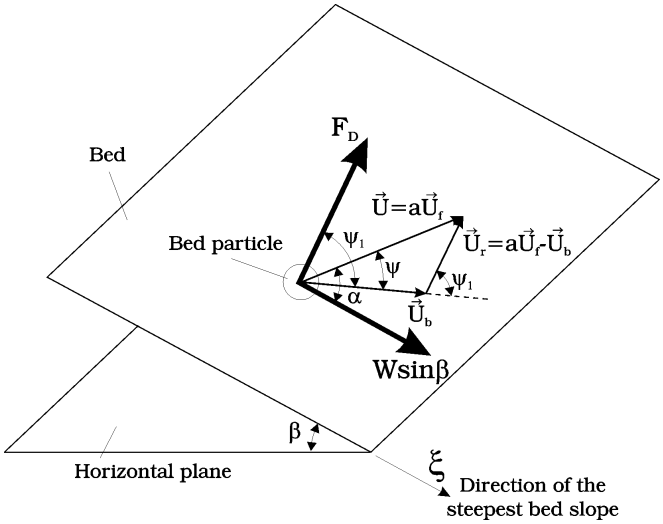

Fig. 3. Force balance on a single bed-load particle on a sloping bed.

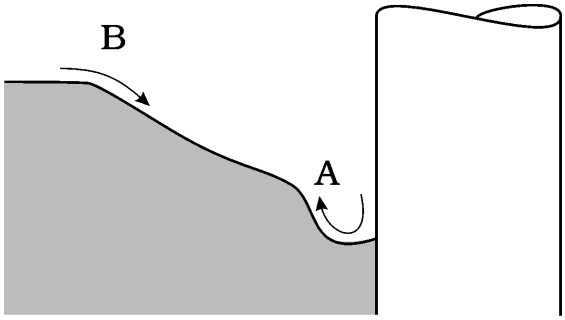

A: Erosion of the foot of the upstream slope
B: Continuous supply of sediment

Fig. 4. Sand slide.

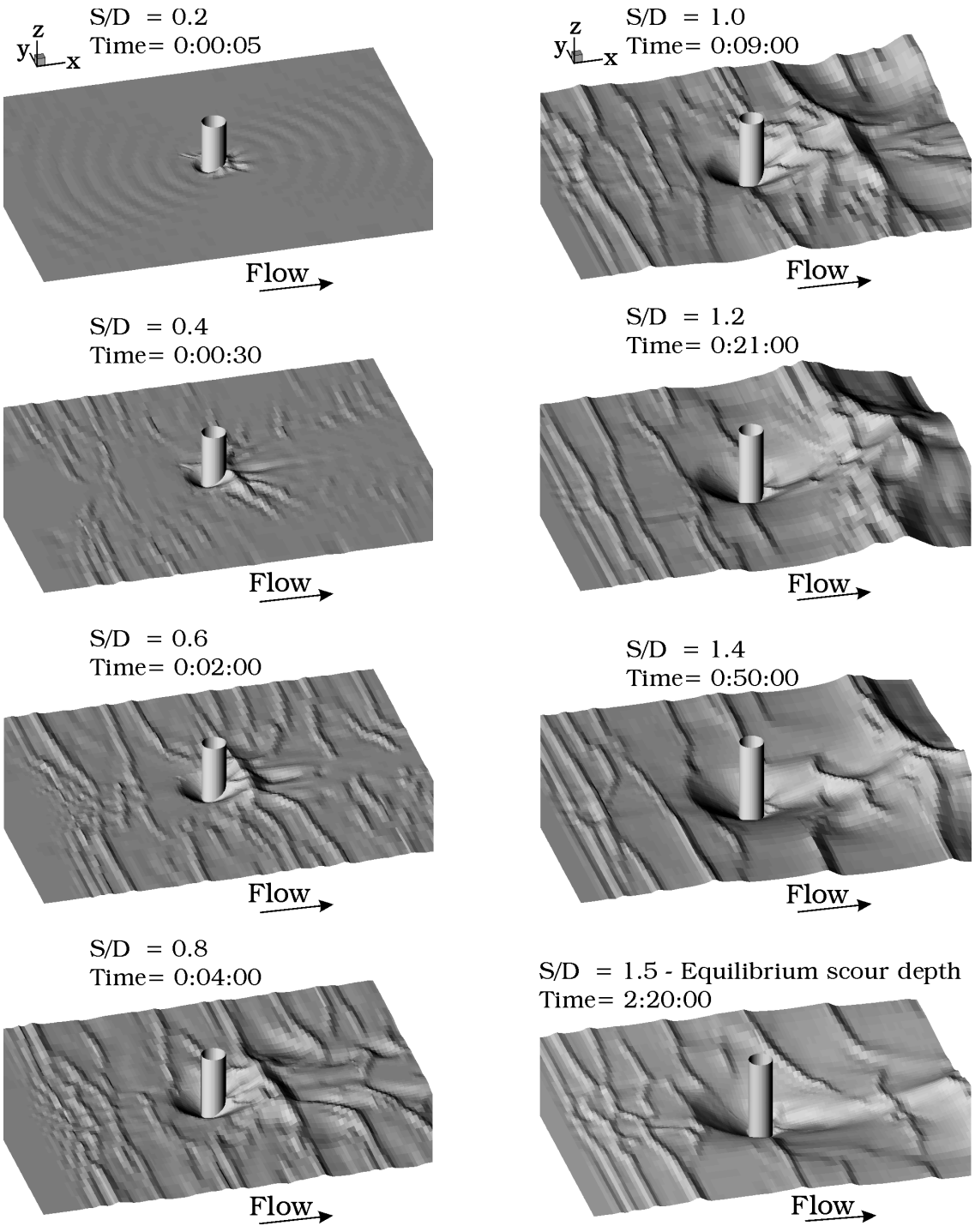

Fig. 5. A sequence of the bed morphology calculated from the present model.

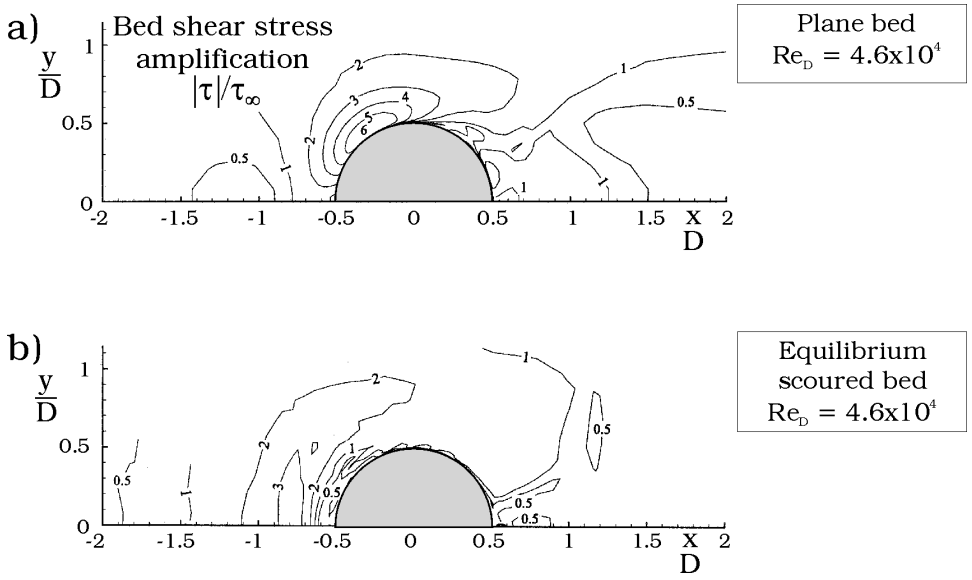

Fig. 6. Amplification in the bed shear stress.

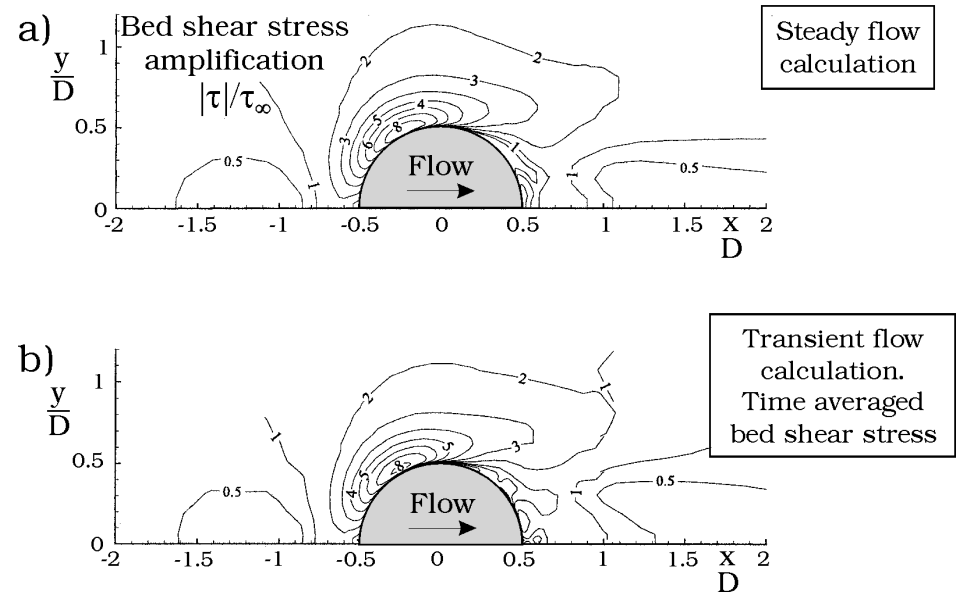

Fig. 7. Amplification in the bed shear stress. Plane bed. Comparison between the steady flow calculation and the transient flow calculation. $Re_D = 4.6\times10^4$, $\delta/D = 2$, $D/k_S = 140$ and $k_S^+ = 15$.